Published in final edited form as:
Cell Mol Bioeng. 2012 December ; 5(4): 493–503. doi:10.1007/s12195-012-0247-6.

A High-Throughput Technique Reveals the Load- and Site Density-Dependent Kinetics of E-Selectin

Jeremy H. Snook and **William H. Guilford**
Department of Biomedical Engineering, University of Virginia, Box 800759, Charlottesville, VA 22908, USA

Abstract

The kinetics of bond rupture between receptors and ligand are critically dependent on applied mechanical force. Force spectroscopy of single receptor-ligand pairs to measure kinetics is a laborious and time-consuming process that is generally performed using individual force probes and making one measurement at a time when typically hundreds of measurements are needed. A high-throughput approach is thus desirable. We report here a magnetic bond puller that provides high-throughput measurements of single receptor-ligand bond kinetics. Electromagnets are used to apply pN tensile and compressive forces to receptor-coated magnetic microspheres while monitoring their contact with a ligand-coated surface. Bond lifetimes and the probability of forming a bond are measured *via* videomicroscopy, and the data are used to determine the load dependent rates of bond rupture and bond formation. The approach is simple, customizable, relatively inexpensive, and can make dozens of kinetic measurements simultaneously. We used the device to investigate how compressive and tensile forces affect the rates of formation and rupture, respectively, of bonds between E-selectin and sialyl Lewis^a (sLe^a), a sugar on P-selectin glycoprotein ligand-1 to which selectins bind. We confirmed earlier findings of a load-dependent rate of bond formation between these two molecules, and that they form a catch-slip bond like other selectin family members. We also make the novel observation of an “ideal” bond in a highly multivalent system of this receptor-ligand pair.

Keywords

Magnetic; Sialyl Lewis; Microscopy; Catch bond; Ideal bond

INTRODUCTION

The relationship between bond kinetics and mechanical force is important in a number of systems, including leukocyte adhesion, tumor metastasis, and actomyosin contraction. The leukocyte adhesion cascade in particular has been extensively characterized, and the steps of cell tethering and rolling are particularly dependent on the rates at which adhesive interactions form and break. Bonds between the selectin family of adhesion proteins and P-selectin glycoprotein ligand-1 (PSGL-1) mediate the kinetics of cell tethering and rolling along the endothelium,[16,20,22,25] and their response to load has been studied in flow chambers[18,23,34,36] and at the single molecule level.[7,11,18,20,28,29,32,33] Though much has been learned, a complete picture of how force affects the time course of bond formation and rupture is still lacking. While many have shown evidence that the selectins form catch

Address correspondence to William H. Guilford, Department of Biomedical Engineering, University of Virginia, Box 800759, Charlottesville, VA 22908, USA. guilford@virginia.edu.

bonds[20,29,31,35]—bonds that last longer with increasing tensile force—we recently presented evidence that force also affects the rate at which bonds form.[31]

Many of these studies entailed measurements of the load-dependent kinetics of single receptor-ligand pairs—a laborious and time-consuming process. Single molecule studies are generally performed by making one measurement at a time. This is true of laser trap studies,[31] as well as similar studies performed with a biomembrane force probe (BFP)[7,18] or an atomic force microscope (AFM).[20,29] While these techniques are effective for measuring the kinetic properties of individual bonds, they are far from efficient. A high-throughput method of measuring data from individual bonds would be invaluable to the field of bond kinetics.

We report here a system that provides high-throughput measurement of single bond kinetics using a variation on a magnetic trap. This approach may be implemented on most microscopes and has been shown previously to achieve forces in the range of tens of pN.[8,12,15,19] The magnetic pulling device is simple, customizable, relatively inexpensive, and can make dozens of kinetic measurements simultaneously. We used the device to investigate how compressive and tensile forces affect the rates formation and rupture, respectively, of bonds between E-selectin and sialyl Lewis^a (sLe^a), a sugar on PSGL-1 to which selectins bind.

MAGNETIC BOND PULLER

The magnetic bond puller consists of electromagnets arranged above and below a flow cell containing paramagnetic microspheres in suspension; the electromagnets are switched on to generate upward and downward forces, respectively. Electromagnets were chosen over permanent magnets due to the difficulty in rapidly changing the field of the later. The force acting on the superparamagnetic beads is modulated by controlling the electromagnet current. During an experiment, the bottom electromagnets are activated to pull the beads into contact with the lower surface of the flow cell (the one bearing ligand) with a specified compressive force for a desired contact time (Fig. 1b). The current in the lower magnets is then turned off, and the current in the top electromagnets magnets simultaneously turned on, applying an upward force on the beads. Beads that failed to form bonds with the surface depart immediately (Fig. 1c), while beads with bonds to the surface depart only after bond rupture (Fig. 1d). The bottom electromagnets are turned back on as the cycle is repeated. The time that each bead spends in contact with the surface is measured by video microscopy (Fig. 1 insets).

Though several geometries can be envisioned, our bond puller consists of four closely spaced electromagnets arranged in a tetrahedron, two above and two below a flow cell (Figs. 2a, 2c). The electromagnet pole faces were machined from 6.6 mm diameter mu-metal rod, a nickel–iron alloy chosen for its high magnetic permeability and low remnant magnetization (Hy-Mu 80, National Electronic Alloys, Santa Ana, CA). Poles were arranged with north and south poles facing one another for both the upper and lower pair of magnets. This produces field lines that move north-to-south across the field of view creating a field gradient that increases from inside the flow cell to the plane of the pole faces. The tip of each pole face was shaped to form a maximum angle of ~55° to prevent flux leakage and generate the maximum possible magnetic field at the tip[13] (Fig. 2b). Each pole tip is placed nearly in contact with the coverslip surface and ~1 mm apart from the opposing pole tip by angling the electromagnet toward the flow cell.

200 turns of copper wire (26 AWG) formed coils 40 mm in length and of 28 mm in outer diameter on a 10 mm spool formed of ABS plastic. Current is supplied by two programmable switching DC power supplies (BK Precision model 1697) that provide up to

40 V and 5 A, and switched *via* a pair of solid state relays under computer control. The transition from open- to close-circuit results in a decaying oscillation in current (Fig. 3a) since the electromagnet and power supply together form a LC resonant circuit. The time from when the off-to-on transition begins until the voltage first reaches the new baseline is 10 ms. After an overshoot, the voltage again reaches the new baseline after an additional 15 ms, while the on-to-off transition occurs in less than 1 ms. Despite the current and field overshoot when load is applied, the time-averaged current over typical activation times is approximately equal to the steady-state current specified by the user.

Device Calibration and Range

The resulting force in the vertical direction, along the optical axis of the microscope, is proportional to the field strength and gradient. To calibrate force as a function of current, we measured the time it took for a bead to arrive at the flow cell surface from the opposite flow cell surface, and calculated force, *f*, using Stokes' formula,

$$f = 6\pi\eta r\nu \quad (1)$$

where η is the fluid viscosity, *r* is the bead radius, and *v* is the bead velocity. With our 3 μm superparamagnetic beads we achieve maximum forces of approximately 40 pN. A force-current calibration curve is shown in Fig. 3b. The force–current relationship is constant to within 4% across the field of view (see supplemental data).

Based on the material properties of mu-metal, as well as the pole face and wire geometry, one can calculate the current at which the poles should saturate according to Ishikawa and Chikazumi.[13] In our system the poles should saturate near a current of 0.6 A, and the force-current curve indeed flattens near this value. The field strength at the tip of each pole face begins to saturate near a current of 0.6 A as well, at which point it has reached 650 Gauss. Because of the low currents we use there are no significant heating effects in the system. Higher forces could be achieved through a number of methods, including increasing bead size, using ferromagnetic beads, or increasing the pole face dimensions.

In our approach to calibration we ignored the contribution of hydrodynamic interactions between the bead and the flow cell surface which will slow departure of the bead from one surface, and slow its approach to the opposing surface. These effects, however, are significant only within a few bead radii of the flow cell surface, while in the bond puller the bead is transiting the entire depth of the flow cell (100 μm). We simulated the departure of a 3 μm bead from a surface at a target electromagnet current of 0.3A. Our simulation included the actual electromagnet current variation over time (Fig. 3a) and corrected for the above-mentioned hydrodynamic interactions according to the equations of Maude.[21] The results of the simulation are shown in Fig. 4. Deviations from constant velocity are only significant in the first ~6 bead radii, or ~18 ms of travel. This is approximately the same as the depth of field of the objective we used, meaning that errors in calibration or measurements due to resonance and hydrodynamic interactions will be negligible. On average the bead is traveling at its terminal velocity.

Data Collection and Analysis

The system is controlled *via* a LabVIEW interface (National Instruments), which allows the user to set the relevant parameters controlling the two pairs of magnets and to view the flow cell surface in real time. The flow cell was imaged through a 0.25 NA 10× objective on an Olympus BH2 microscope with bright field illumination and a digital CCD camera (Allied Vision Technologies, GC655) operating at 90 frames per second. The intensity of a single

pixel in each image of the digitally recorded video is changed to indicate whether the magnets are pulling up or down at any instant in time.

Bond formation and rupture is tracked using a custom plugin for ImageJ[27] based on the Mtrack2 plugin by Nico Stuurman (UCSF). The user sets a threshold that selects beads. The plugin tracks all microspheres, filtering out those that do not meet specified criteria for size and circularity. It treats each up-down sequence as a cycle and ignores particles that were on the flow cell surface prior to the current cycle. The beginning and end of each cycle is determined by monitoring the value of the pixel altered by LabView (see previous paragraph). During the period of time when compressive force is applied, the number of frames between when a microsphere appears on the surface and when the force direction is reversed provides the contact time for each microsphere. Once force is reversed to the tensile direction the plugin monitors the time the microsphere remains in contact with the surface. If a microsphere disappears or moves more than a threshold distance in a single frame, it is considered no longer bound and its bond lifetime is recorded as the time since the transition to tensile force. Microspheres that remain on the surface for more than one cycle are considered irreversibly bound, and are recorded for adhesion probability measurements but not used for bond lifetime measurements. The plugin saves arrays of contact times under compressive force, bond lifetimes under tensile force, the number of particles per cycle, and the adhesion probability.

Temporal Resolution

The temporal resolution of the bond puller is a function not only of the frame rate of the digital camera used to record bead arrivals and departures (90 frames/s in this instance), but of the axial, out-of-plane resolution of the imaging system. The latter sets the limit on how close or far a bead must be from the flow cell surface to be detected as in contact, or unbound, respectively.

Depth of field (z) was used as an estimate of this limit, and is given by

$$z = 2\lambda n / NA^2 \quad (2)$$

where λ is the imaging wavelength, n is the refractive index of the medium, and NA is the numerical aperture of the microscope objective. The 0.25 NA objective used in this study provides a depth of field of ~9 μm. If one assumes that any bead within the depth of field will appear to be on the surface, this means that a bead will have to be at least 9 μm off the surface of the flow cell in order to detect that it is no longer bound. The time required for a bead to be pulled 9 μm off the surface depends on the magnitude of the force pulling on it, and this sets the minimum bond lifetime we are able to detect, $t_{\min}$.

$$t_{\min} = 6\pi\eta r z / f_t \quad (3)$$

where η is the fluid viscosity, r is the bead radius, and f_t is the applied tensile load. The minimum detectable bond lifetime for our current arrangement ranges from 51 ms at 5 pN to 6 ms at 40 pN. The same principal applies to compressive load (f_c). Since bead arrivals are not perfectly uniform we track arrival times individually so that we may individually calculate contact times. As a bead is pulled toward the ligand-coated surface, it will appear to arrive up to $t_{\min}$ earlier than actual contact, and will thus make the contact time appear longer than it actually is. This will introduce a relative error that is larger both for small f_c, since beads will penetrate the depth of field more slowly, and for small contact times since the uncertainty in arrival times will be a larger fraction of the desired contact time. These errors are illustrated in Fig. 5.

Regardless, the frame rate of the camera sets the absolute lower bound on temporal resolution, to 11 ms in this instance, or 22 ms by the Nyquist criterion.

Though the time for compressive force application is set by the user, the actual arrival times for beads coming into contact with the ligand-coated surface vary (Fig. 6). This variation is the result of a number of factors, including short-lived non-specific bonds with the blocked surface, small force variations across the field of view, and beads that never made it all the way back to the blocked surface prior to next force cycle, and thus had a shorter distance to travel to reach the ligand-coated surface. These phenomena result in a distribution of contact time measurements even for single setting. Though this necessitates the tracking of each individual bead history, it further increases the throughput of contact time measurements and associated adhesion probability experiments.

METHODS

Superparamagnetic 3 μm beads (Bangs Laboratories, Fishers, IN) were covalently coupled to chimeric recombinant human E-selectin (R&D Systems, Minneapolis, MN) as previously described.[3,31] 20 μL (10% solids) of beads were suspended in 1 mL of 50 mM MES, pH 6.1 (MES activation buffer). Beads were washed by centrifugation three times with 1 mL MES activation buffer and resuspended in 50 μL activation buffer following the final wash. Next, 500 μL of 200 mM NHS was added while mixing, followed by 500 μL of 4% (w/v) EDAC. This was allowed to react for 30 min at room temperature on a circular rotator. Beads were then washed twice with 1 mL of 50 mM MES, pH 7.4 (MES coupling buffer) and were resuspended in 100 μL MES coupling buffer following the final wash. 25 μL of 1 mg/mL E-selectin was added to the beads and they were rotated overnight at 4°C. Beads were then washed twice with 1 mL of MES coupling buffer and resuspended in 1 mL of 0.1 M ethanolamine, followed by rotation for 30 min at room temperature to block un-reacted sites. Beads were then washed twice with 1 mL of "flow cell buffer" (150 mM NaCl, 25 mM Imidazole, 1 mM $CaCl^{1,2}$ mM NaN_3, pH 7.4), resuspended in 1 mL of flow cell buffer with 0.5% Tween-20 for blocking, and rotated at room temperature for 1 h. Beads are stored at 4°C.

Flow cells were prepared using 0.1 mm thick mylar shims to separate a 22 × 22 mm glass coverslip from an 18 × 18 mm glass coverslip, forming a ~ 25 μL chamber. Two flow cells were made for each experiment. In one flow cell, 10 mg/mL mPEG-Silane (MW 5000, Laysan Bio, Arab, AL) in acetonitrile was incubated for 1 h. Avidin was then incubated at 200 μg/mL in the flow cell for one hour in 10 mg/mL mPEG-Silane in double distilled H_2O. Next, sLe_a-PAA-biotin (Glycotech, Rockville, MD) was incubated at 100 μg/mL for 15 min. In the second flow cell, 10 mg/mL mPEG-Silane in acetonitrile was incubated for one hour. Thus, while both flow cells were blocked with PEG, one flow cell also had two sLe_a-bearing surfaces. The two flow cells were split apart and recombined to make two new flow cells, each containing one coverslip from each of the originals. Each new flow cell thus had one blocked surface and one sLe_a-bearing surface. E-selectin-bound beads where then added to each flow cell and used immediately for experiments.

RESULTS

The Rate of Bond Formation Between E-Selectin and sLe^a is Load-Dependent

The fraction of contacts forming a bond ("adhesion probability", $p(t)$) can be plotted as a function of contact time to determine on-rates—that is, the forward reaction rate between a receptor and its ligand. Adhesion probability can then be used to estimate the rate of bond formation, as in Chesla *et al*.[5] We fitted

$$p(t) = 1 - \exp\{-m_r m_l A_c K_a^o (1 - \exp(-k_{off}^o t))\} \quad (4)$$

where K_a^o is the equilibrium binding affinity (k_{on}^o / k_{off}^o), m_r and m_l are the measured site densities of receptors and ligands, and A_c the estimated contact area. The specific 2-D on-rate, k_{on}^o, was calculated from the fitted values of k_{off}^o and $m_r m_l A_c K_a^o$. This was done for different compressive forces to determine the effect of compressive force on 2-D on-rate. These experiments were done at a high site density to ensure that k_{on}^o is a measure of the rate of molecular adhesion, rather than a measure of the rate of diffusion between the opposing surfaces. As seen in Fig. 7a, adhesion probability increases with increasing contact time for interactions at all forces, eventually reaching similar saturating values. As compressive force is increased, the adhesion probability curve shifts left and approaches saturation at a shorter contact time. These data are summarized in Fig. 7b which shows that effective 2-D on-rate ($m_r m_l A_c k_{on}^o$) increases with increasing compressive force. This confirms our previous results from laser trap experiments.[31]

The Apparent Load-Dependence of Bond Rupture Depends on Site Density

When the system switches from compressive to tensile loads, we get a measure of load-dependent bond lifetime. Measurements of bond lifetime over a range of tensile loads at the same high site density as above showed little effect of force on bond lifetime (Fig. 8a). This is in contrast to previous laser trap data showing a catch-slip bond between E-selectin and sLe^a with a peak lifetime at 30 ± 14 pN.[31] The lifetimes measured here across all forces average 1420 ms, which is similar to the peak lifetime of 1280 ms (at 30 pN) found previously. For an exponential distribution of bond lifetimes the standard deviation should be equal to the mean bond lifetime; indeed, they are approximately equal in our measurements, and still demonstrate a relatively flat response to tensile load.

We hypothesized that longer than expected lifetimes at low forces were due to the high site density which may cause either (a) a multiplicity of initial bonds, or (b) formation of new bonds, even as tensile load is being applied. To test this hypothesis we repeated the bond lifetime experiments using a 1000-fold lower concentration of sLe^a such that we would be likely to measure true single molecule adhesions. At this lower site density the adhesion probability was reduced from an average of 58% to an average of 25% at which ~80% of bonds are expected to be single bonds.[5] Results for bond lifetime measurements over a range of tensile forces (Fig. 8b) show bond lifetime to first increase with tensile force and then decrease as force is increased further, characteristic of a catch-slip bond. The critical force occurs at 22 ± 14 pN at a peak lifetime of 1050 ms as determined by a fit of the two-pathway catch-slip model to the data.[24] Both of these values are somewhat lower than yet similar to those we found previously using the laser trap[31] in which we likewise observed catch-slip behavior.

DISCUSSION

The magnetic bond puller is capable of applying highly tunable vertical forces to dozens of beads simultaneously, allowing kinetic data on single bond association and dissociation rates to be determined with much greater throughput than with previous methods. Its low cost and simple design make it adaptable to virtually any microscope and a number of experimental systems. The ability to rapidly acquire kinetic information in an automated fashion makes the device a potentially powerful tool in the broader field of molecular biomechanics. We demonstrate its use by measuring the effect of force on the 2-D kinetics of E-selectin and sialyl Lewis^a, and confirm previous observations from the laser trap of catch-slip behavior in

bond rupture, and compressive load-dependent rates of bond formation. We also find evidence of load-independent rates of bond rupture when ligand site densities are high.

Bond Kinetics

These data highlight the importance of measuring adhesion probability when attempting to conduct single molecule bond lifetime experiments. Though adhesion probability experiments must be performed at high site density to avoid the limitations of convective and diffusive transport of ligand to receptor, bond lifetime experiments should generally be performed at site densities low enough to assure a high fraction of single bond events; otherwise details of the single-molecule energy landscape may be lost.

Nonetheless, our observation of load-independent bond lifetimes is interesting and potentially of broad physiological importance. Bond lifetimes that are independent of tensile load are characteristic of an "ideal" bond.[6] Experiments repeated at a lower site density, however, show a catch-slip bond with a critical force of ~22 pN. Taken together, these observations suggest that "ideal bonds" may appear if experiments are performed at site densities where the likelihood of multivalent interactions or rebinding (formation of new bonds) is high. In leukocyte rolling, periods of high selectin expression likely result in highly multi-valent interactions between selectins and their ligands. This may cause a collection of individual catch bonds to manifest as a single ideal bond, and allow rolling to occur over a broad range of shear stress.

The increase in association rate between E-selectin and sialyl Lewis^a with increasing compressive force is a relationship similar to that found previously by us using a laser trap.[31] While the average magnitudes of the on-rates are ~2-fold lower than those found with a laser trap (17.5 s^{-1} vs. 29.7 s^{-1}, respectively), the degree to which they depend on compressive force is similar. The laser trap data showed 2-D on-rate to increase ~5-fold as compressive force increased from 6 to 46 pN, while the magnetic puller data showed on-rate to increase ~4-fold as compressive force increased from 6 to 39 pN. The differences in measured on-rate can likely be attributed to the use of different blocking techniques in the different experimental systems. The good agreement between data obtained *via* two completely different experimental approaches provides strong evidence that rates of association between E-selectin and sLe^a do, in fact, increase with increasing compressive force.

We previously considered four physical models to explain the load-dependent on-rates we measured with the laser trap,[31] and the current work lends further evidence to our conclusion that it is the result of a "reverse Bell model," whereby compressive force causes the molecules to bind faster by tilting the energy landscape and thus reducing the activation energy for binding. This requires the opposing binding sites to be approximately opposite one another prior to contact, at which point force causes a direct enhancement of binding rate. This is analogous to the Bell model for force-induced dissociation, but with the energy landscape tilting in the opposite direction.

$$k_{\mathrm{on}}(f_{\mathrm{c}}) = k_{\mathrm{on}}^{\mathrm{o}} \exp\left(f_{\mathrm{c}} \cdot x_{\gamma \mathrm{a}} / k_{\mathrm{B}} T\right) \quad (5)$$

where $k_{\mathrm{on}}(f_{\mathrm{c}})$ is the load-dependent on-rate, $k_{\mathrm{on}}^{\mathrm{o}}$ is the unloaded on-rate, f_{c} the applied compressive load, $x_{\gamma \mathrm{a}}$ the characteristic bond length of association, k_{B} the Boltzmann constant, and T the absolute temperature. Fitting this model to our data yields a $k_{\mathrm{on}}^{\mathrm{o}}$ of 8 ± 1 s^{-1} and an $x_{\gamma \mathrm{a}}$ of 0.14 ± 0.02 nm, which compare well with the $k_{\mathrm{on}}^{\mathrm{o}}$ of 8.2 ± 0.9 s^{-1} and $x_{\gamma \mathrm{a}}$ of 0.19 ± 0.03 nm we found previously using the laser trap. If this model is indeed correct, all bonds should exhibit load-dependent on-rates regardless of how their lifetimes are effected by tensile load. A mechanism involving a conformational change of the hinge region is also

a possibility, and performing similar tests with selectin mutants possessing a modified hinge region may be informative.

Though the rates of bond formation and rupture measured here differ from our earlier data from the laser trap, these differences are unlikely to be meaningful. Average lifetimes vary greatly by experimental technique, and it is the trend in lifetimes that is of particular interest. For example, a recent study found peak average lifetimes of E-selectin/sialyl Lewis^x bonds to vary by nearly 4-fold when measured with a biomembrane force probe vs. a flow chamber.[35]

Magnetic Bond Puller

The magnetic bond puller has significant advantages over other probe-based approaches to force spectroscopy. The most significant of these is that unlike other approaches that yield one measurement per touch-pull cycle, the magnetic bond puller typically generates dozens of kinetic measurements per cycle, and so yields hundreds of measurements during an experiment lasting only a few minutes. It does not suffer the optical artifacts that plague the laser trap approach,[9,26,31] and is considerably less expensive to implement. It also samples a smaller contact area than a recently reported chip-based assay[30] and can apply forces at much higher rate than centrifugal assays.[10]

There are, nonetheless, several cautions to prospective users and limitations of which they should be aware. For example, superparamagnetic beads have a high magnetic susceptibility, and the constantly applied magnetic field does not allow the beads to demagnetize between cycles of an experiment. This results in bead aggregation due to mutual attraction. This problem can be partially overcome by moving the flow cell during the experiment to find regions where bead clumping is minimal, but it remains a significant limitation to the throughput of the technique. Magnetic interactions between single beads are not, however, a significant limitation in individual calibrations for force measurements. The interaction force between two beads in a uniform field is estimated to be only 1.2 pN at our highest current when the bead separation distance is two bead diameters.[1,2,14,17] While this is sufficient to cause beads to aggregate over several pull cycles, it is not enough to significantly affect the biological results.

Another limitation is that the pulling direction is not perfectly vertical, but rather varies over the field of view. While the system pulls in a vertical direction near the center of the field, in fringe areas the pulling angle with the flow cell surface can be as low as ~45°. For a bead tethered to the flow cell surface by a single bond, when the pulling angle is below a critical angle, θ_{crit}, the bead will likely be in contact with the flow cell surface while tensile force is being applied. The critical angle $\theta_{crit} = \sin^{-1}(r/(r + l))$, where r is the bead radius and l is the bond length, is 74° for our system. With an average pulling angle of 67° in our measurements, a significant fraction of beads will have tilted into contact with the surface while undergoing tensile load. This will cause a lever effect on the beads that may result in a small (<10%) overestimation of tensile force. This concern could be alleviated by tracking only beads near the center of the field of view. Alternatively, a more uniform field could be generated using a more complex array of electromagnets.

Unlike laser trap experiments, the magnetic bond puller doesn't allow one to detect the moment when a bond forms or to detect whether single or multiple bonds are breaking. Rather, one can only measure when the last bond ruptures. Thus while laser traps and atomic force spectroscopy can directly measure on-rate by monitoring initial bond formation,[4,31] with the magnetic bond puller one must use the indirect approach of measuring adhesion probability as a function of contact time.[5] Thus the magnetic pulling system lacks the

richness of experimental data that can be obtained from considerably more expensive high-throughput systems, like the automated force "spectroscope."[29]

A final limitation of the magnetic pulling system is the error associated with measuring contact time and bond duration. It is not possible to detect the exact moment at which a bead comes into contact with or leaves the surface. Rather, the tracking program designates a bead as being on the surface when it is approximately within the depth of field. This results in an overestimate of contact time and bond duration. Because lower applied forces result in slower bead velocities, beads pulled with lower forces spend a longer time in the depth of field, and consequently have larger overestimates of contact time and bond duration than similarly behaving beads pulled with higher forces. This error is more critical in measuring contact times than bond durations because bond durations are many fold longer than contact times. Manual measurements of contact time and bond duration were made at low forces to get a more accurate estimate of these parameters. At extremely low forces (<10 pN), there is likely still small error in the measurement due to the difficulty in determining exactly when a bead comes into contact with or leaves contact with the surface, even with manual measurement.

A significant improvement in the accuracy of contact time and bond lifetime measurements could be accomplished by using an objective with a higher NA. For example, an increase in NA from the current 0.25–0.35 will lower the depth of field from 9 to 3 μm, significantly lowering the minimum detectable bond lifetime (Fig. 5b); a 1.0 NA objective will obviously perform even better, though getting the pole faces in place with a water- or oil-immersion objective will prove challenging. An attractive alternative is to design the magnets to work on a total internal reflection (TIRF) microscope, in which case the resolution of bead-surface contact would be exceptional—on the order of half a wavelength. A camera with a higher frame rate would also improve measurement accuracy at high forces by allowing detection of the shortest of bonds.

Acknowledgments

The authors wish to express their thanks to Mr. Alexander McClure for his assistance with magnet assembly, and Dr. Alexander Klibanov of the University of Virginia for his advice on surface passivation. This work was supported by the National Institutes of Health (EB002185).

REFERENCES

1. Baselt DR, Lee GU, Natesan M, Metzger SW, Sheehan PE, Colton RJ. A biosensor based on magnetoresistance technology. Biosens. Bioelectron. 1998; 13:731–739. [PubMed: 9828367]
2. Besse PA, Boero G, Demierre M, Pott V, Popovic R. Detection of a single magnetic microbead using a miniaturized silicon Hall sensor. Appl. Phys. Lett. 2002; 80:4199–4201.
3. Brunk DK, Hammer DA. Quantifying rolling adhesion with a cell-free assay: E-selectin and its carbohydrate ligands. Biophys. J. 1997; 72:2820–2833. [PubMed: 9168056]
4. Chen W, Evans EA, McEver RP, Zhu C. Monitoring receptor-ligand interactions between surfaces by thermal fluctuations. Biophys. J. 2008; 94:694–701. [PubMed: 17890399]
5. Chesla SE, Selvaraj P, Zhu C. Measuring two-dimensional receptor-ligand binding kinetics by micropipette. Biophys. J. 1998; 75:1553–1572. [PubMed: 9726957]
6. Dembo M, Torney DC, Saxman K, Hammer D. The reaction-limited kinetics of membrane-to-surface adhesion and detachment. Proc. R. Soc. Lond. B Biol. Sci. 1988; 234:55–83. [PubMed: 2901109]
7. Evans E, Leung A, Heinrich V, Zhu C. Mechanical switching and coupling between two dissociation pathways in a P-selectin adhesion bond. Proc. Natl Acad. Sci. USA. 2004; 101:11281–11286. [PubMed: 15277675]

8. Gosse C, Croquette V. Magnetic tweezers: micro-manipulation and force measurement at the molecular level. Biophys. J. 2002; 82:3314–3329. [PubMed: 12023254]
9. Guo B, Guilford WH. Mechanics of actomyosin bonds in different nucleotide states are tuned to muscle contraction. Proc. Natl Acad. Sci. USA. 2006; 103:9844–9849. [PubMed: 16785439]
10. Halvorsen K, Wong WP. Massively parallel single-molecule manipulation using centrifugal force. Biophys. J. 2010; 98:L53–L55. [PubMed: 20513382]
11. Hanley WD, Wirtz D, Konstantopoulos K. Distinct kinetic and mechanical properties govern selectinleukocyte interactions. J. Cell Sci. 2004; 117:2503–2511. [PubMed: 15159451]
12. Huang H, Dong CY, Kwon HS, Sutin JD, Kamm RD, So PTC. Three-dimensional cellular deformation analysis with a two-photon magnetic manipulator workstation. Biophys. J. 2002; 82:2211–2223. [PubMed: 11916876]
13. Ishikawa Y, Chikazumi S. Design of high power electromagnets. Jpn. J. Appl. Phys. 1962; 1:155–173.
14. Keaveny EE, Maxey MR. Modeling the magnetic interactions between paramagnetic beads in magnetorheological fluids. J. Comput. Phys. 2008; 227:9554–9571.
15. Kollmannsberger P, Fabry B. High-force magnetic tweezers with force feedback for biological applications. Rev. Sci. Instrum. 2007; 78:114301. [PubMed: 18052492]
16. Ley K. Molecular mechanisms of leukocyte rolling and adhesion to microvascular endothelium. Eur. Heart J. 1993; 14:68–73. [PubMed: 8293782]
17. Liu D, Maxey MR, Karniadakis GE. Simulations of dynamic self-assembly of paramagnetic microspheres in confined microgeometries. J. Micromech. Microeng. 2005; 15:2298–2308.
18. Lou J, Yago T, Klopocki AG, Mehta P, Chen W, Zarnitsyna VI, Bovin NV, Zhu C, McEver RP. Flow-enhanced adhesion regulated by a selectin interdomain hinge. J. Cell Biol. 2006; 174:1107–1117. [PubMed: 17000883]
19. Maier B, Bensimon D, Croquette V. Replication by a single DNA polymerase of a stretched single-stranded DNA. Proc. Natl Acad. Sci. USA. 2000; 97:12002–12007. [PubMed: 11050232]
20. Marshall BT, Long M, Piper JW, Yago T, McEver RP, Zhu C. Direct observation of catch bonds involving cell-adhesion molecules. Nature. 2003; 423:190–193. [PubMed: 12736689]
21. Maude AD. End effects in a falling-sphere viscometer. Br. J. Appl. Phys. 12:293–1961.
22. McEver RP, Moore KL, Cummings RD. Leukocyte trafficking mediated by selectin-carbohydrate interactions. J. Biol. Chem. 1995; 270:11025–11028. [PubMed: 7538108]
23. Paschall CD, Guilford WH, Lawrence MB. Enhancement of L-selectin, but not P-selectin, bond formation frequency by convective flow. Biophys. J. 2008; 94:1034–1045. [PubMed: 17890384]
24. Pereverzev YV, Prezhdo OV, Forero M, Sokurenko EV, Thomas WE. The two-pathway model for the catch-slip transition in biological adhesion. Biophys. J. 2005; 89:1446–1454. [PubMed: 15951391]
25. Ramos CL, Kunkel EJ, Lawrence MB, Jung U, Vestweber D, Bosse R, McIntyre KW, Gillooly KM, Norton CR, Wolitzky BA, Ley K. Differential effect of E-selectin antibodies on neutrophil rolling and recruitment to inflammatory sites. Blood. 1997; 89:3009–3018. [PubMed: 9108422]
26. Rao VS, Clobes AM, Guilford WH. Force spectroscopy reveals multiple “closed states” of the muscle thin filament. J. Biol. Chem. 2011; 286:24135–24141. [PubMed: 21597115]
27. Rasband, WS. NIH Image, ImageJ. 1997.
28. Rinko LJ, Lawrence MB, Guilford WH. The molecular mechanics of P- and L-selectin lectin domains binding to PSGL-1. Biophys. J. 2004; 86:544–554. [PubMed: 14695299]
29. Sarangapani KK, Yago T, Klopocki AG, Lawrence MB, Fieger CB, Rosen SD, McEver RP, Zhu C. Low force decelerates L-selectin dissociation from P-selectin glycoprotein ligand-1 and endoglycan. J. Biol. Chem. 2004; 279:2291–2298. [PubMed: 14573602]
30. Severin PM, Ho D, Gaub HE. A high throughput molecular force assay for protein-DNA interactions. Lab. Chip. 2011; 11:856–862. [PubMed: 21221429]
31. Snook JH, Guilford WH. The effects of load on E-selectin bond rupture and bond formation. Cell. Mol. Bioeng. 2010; 3:128–138. [PubMed: 20526425]
32. Sun GY, Zhang Y, Huo B, Long MA. Parametric analysis for monitoring 2D kinetics of receptor-ligand binding. Cell. Mol. Bioeng. 2009; 2:495–503.

33. Tees DF, Waugh RE, Hammer DA. A micro-cantilever device to assess the effect of force on the lifetime of selectin-carbohydrate bonds. Biophys. J. 2001; 80:668–682. [PubMed: 11159435]

34. Waldron TT, Springer TA. Transmission of allostery through the lectin domain in selectin-mediated cell adhesion. Proc. Natl Acad. Sci. USA. 2009; 106:85–90. [PubMed: 19118202]

35. Wayman AM, Chen W, McEver RP, Zhu C. Triphasic force dependence of e-selectin/ligand dissociation governs cell rolling under flow. Biophys. J. 2010; 99:1166–1174. [PubMed: 20713000]

36. Yago T, Wu J, Wey CD, Klopocki AG, Zhu C, McEver RP. Catch bonds govern adhesion through L-selectin at threshold shear. J. Cell Biol. 2004; 166:913–923. [PubMed: 15364963]

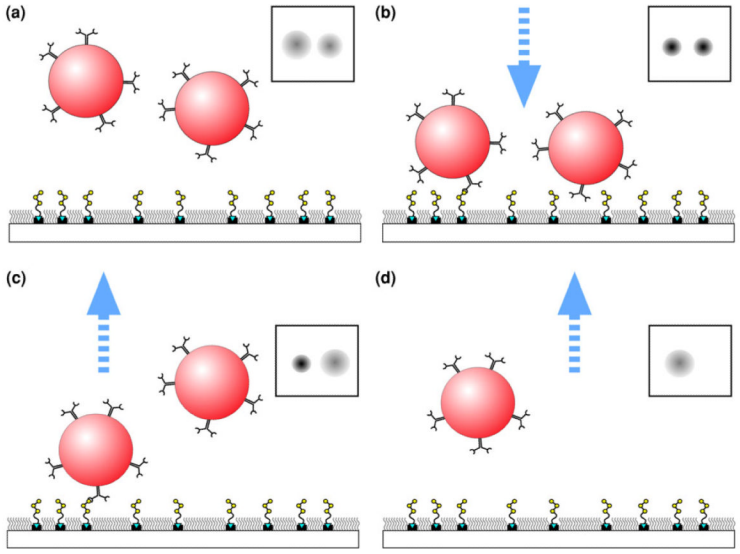

FIGURE 1.

Bead locations and resulting images (insets) for a cycle of measurement in the magnetic bond puller. Beads are first near the surface and can be faintly seen in image (a). Downward force is applied, pulling beads into contact with the surface and resulting in dark spots in image (b). Upward force is then applied. Beads that had not formed a bond move upward immediately, while beads that had formed a bond remain on the surface until bond rupture (c). After bonds have ruptured, all beads are now off the surface and no spots remain the image (d).

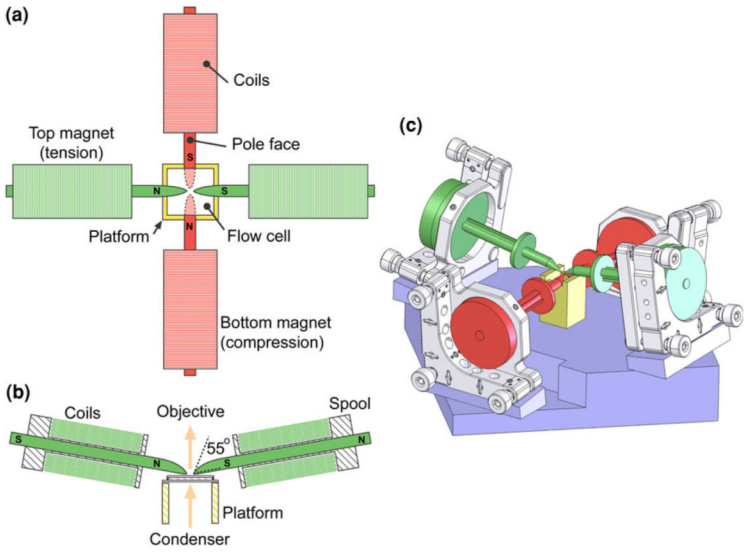

FIGURE 2.

Magnetic puller design. (a) Top and (b) side view of magnetic puller show the four mu-metal rods oriented at 90° angles around a flow cell, which is supported on a pedestal (yellow). Two rods are angled from above (green) and two rods are angled from below (red) in order to provide upward and downward force, respectively. Rods coming from below are omitted from side view. (c) Isometric view of assembly, including the supporting stage (blue). The electromagnet coils are not shown.

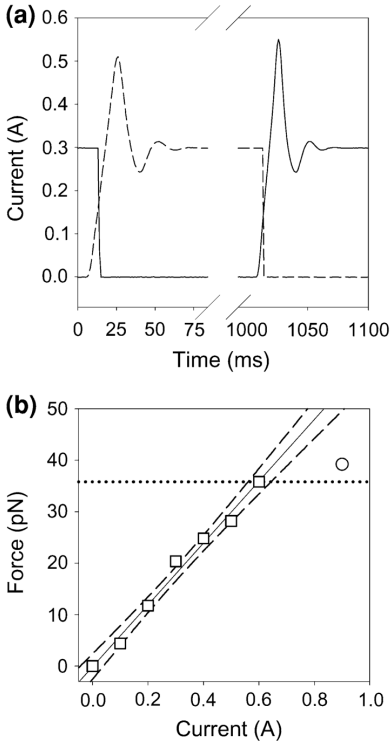

FIGURE 3.

Characterization and calibration of the electromagnets. (a) Voltage over one representative cycle of the magnetic pulling system. The dashed line represents the down-pulling magnets and the solid line represents the up-pulling magnets. (b) Calibration curve showing applied force as a function of current. Solid line is a best fit line to all measured calibration points excluding those at 0.9 A. Dashed lines are 95% confidence intervals of the best fit line. Data at 0.9 A was excluded from the fit as it was analytically determined that the relationship between force and current should not be linear above currents of 0.6 A (see text). The horizontal dotted line indicates the predicted point of saturation.

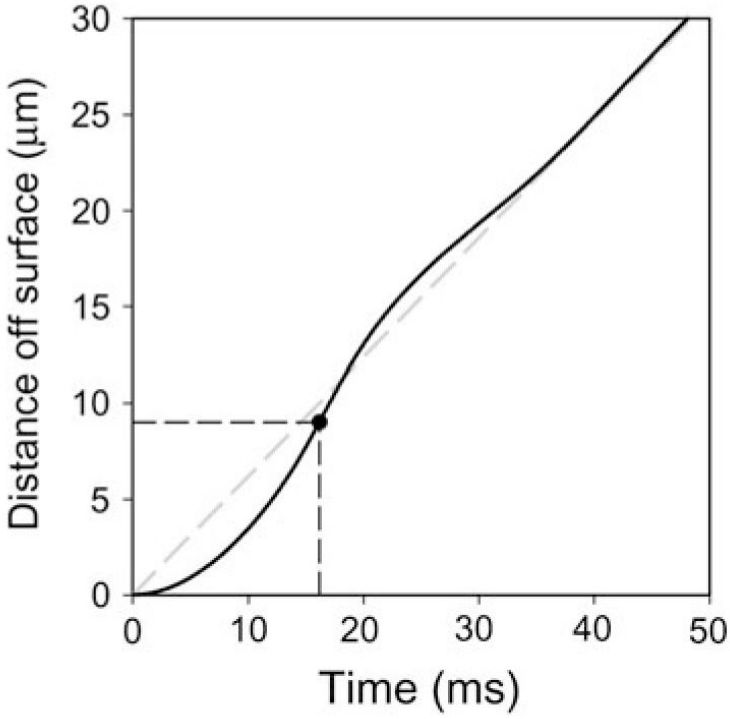

FIGURE 4.

Theoretical time course of bead displacement from the flow cell surface. A current of 0.3A is initiated at time zero. The simulation accounts for the resonance in current seen in Fig. 3a and the hydrodynamic interaction between the surface and the microsphere.[21] The drop lines indicate the time at which the depth of field is reached. The dashed line shows the ideal displacement at constant velocity. Note that the two lines converge near the depth of field.

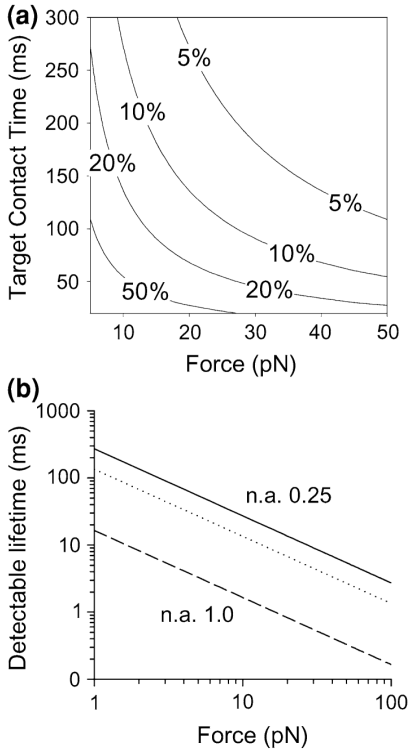

FIGURE 5.

Fundamental limits of accuracy in contact time and bond lifetime measurements. (a) Percent error in determining the bead-surface contact time as a function of force and target contact time. This assumes a 0.25 NA, 10× air objective imaging 3 μm beads in an aqueous medium, as used here. (b) Minimum detectable bond lifetime as a function of applied force. Relationships are shown for a 0.25 NA, 10× air objective, as used here, a 0.35 NA objective (dotted line), and a 1.0 NA objective (dashed line).

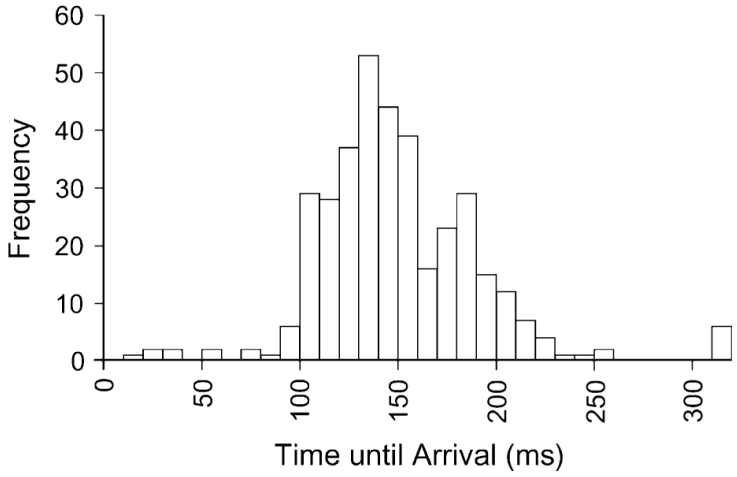

FIGURE 6.
Histogram showing the times from initiation of compressive force until arrival of individual beads on the ligand-coated surface for a force of 18 pN.

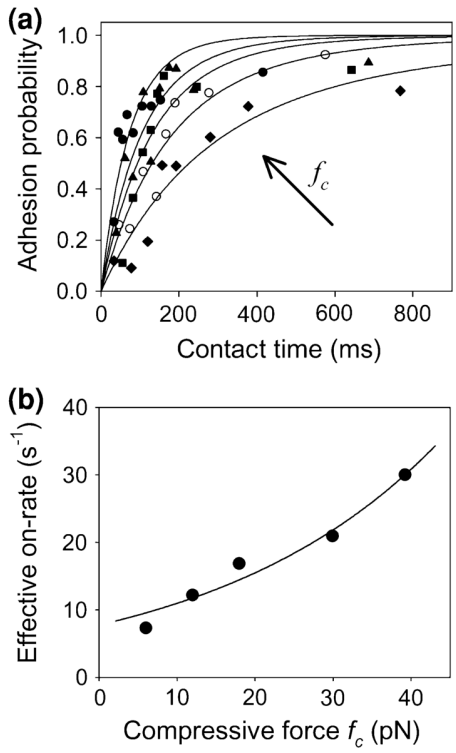

FIGURE 7.

Measuring compressive force-dependent rates of bond formation. (a) Probability of bond formation as a function of contact time for compressive forces of 6 pN (◆), 12 pN (), 18 pN (), 30 pN (), and 39 pN (●). Data are cumulative sums of total adhesions divided by total contacts at each contact time. Lines are fits to Eq. (4) for each of the forces, separately. (b) Effective 2-D on-rate as a function of compressive force. Line is a fit of the reverse Bell model (Eq. (5)).

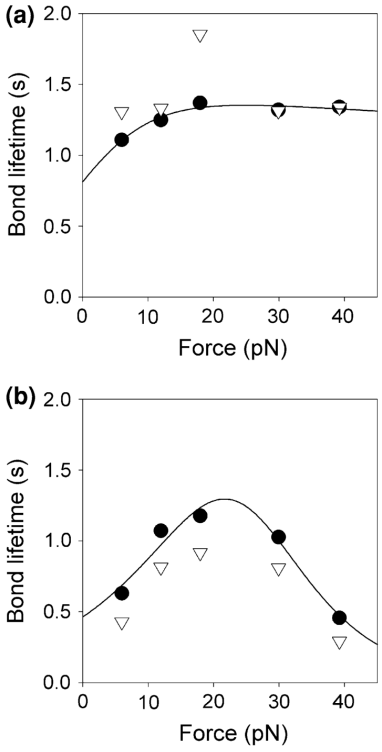

FIGURE 8.

Bond lifetime as a function of tensile force. Mean bond lifetimes (▿) and standard deviation of bond lifetimes (.) are shown for each force at high site density (a) and low site density (b). Each is fitted by a two-pathway model for catch-slip adhesion,[24] though at high site densities the fit yields unrealistic values.